TITLE

Proximity labeling reveals dynamic changes in the SQSTM1 protein network

Alejandro N. Rondón Ortiz [1,2,3], Lushuang Zhang [3], Peter E.A. Ash [3], Avik Basu [2,4,5], Sambhavi Puri [3], Sophie J.F. van der Spek [3], Luke Dorrian [3], Andrew Emili [2,4,5*], Benjamin Wolozin [3,6,7,8,9*]

[1] Department of Biology, Boston University, Boston, MA 02215, USA

[2] Center for Network Systems Biology, Boston University, Boston, MA 02215, USA

[3] Departments of Anatomy & Neurobiology, Boston University, Boston, MA 02215, USA

[4] Department of Biochemistry, Boston University, Boston, MA 02115, USA

[5] Department of Chemical Physiology & Biochemistry, Oregon Health Sciences University, Portland, OR 97239, USA

[6] Center for Systems Neuroscience, Boston University, Boston, MA 02115, USA

[7] Center for Neurophotonics, Boston University, Boston, MA 02115, USA

[8] Department of Neurology, Boston University, Boston, MA 02115, USA

[9] Department of Pharmacology, Physiology and Biophysics

*Corresponding Authors:

bwolozin@bu.edu

emili@ohsu.edu

ABSTRACT

Sequestosome1 (SQSTM1) is an autophagy receptor that mediates degradation of intracellular cargo, including protein aggregates, through multiple protein interactions. These interactions form the SQSTM1 protein network that are mediated by SQSTM1 functional interaction domains, which include LIR, PB1, UBA and KIR. Despite various attempts to unravel the complexity of the SQSTM1 protein network, our understanding of the relationship of various components in cellular physiology and disease states continues to evolve. To investigate the SQSTM1 protein interaction network, we performed proximity profile labeling by fusing TurboID with the human protein SQSTM1 (TurboID::SQSTM1). This chimeric protein displayed well-established SQSTM1 features including: production of SQSTM1 intracellular bodies, binding to known SQSTM1 interacting partners via defined functional SQSTM1 interacting domains and capture of novel SQSTM1 interactors. Strikingly, aggregated tau protein altered the protein interaction network of SQSTM1 to include many stress-associated proteins. Overall, our work reveals the dynamic landscape of the SQSTM1 protein network and offers a resource to study SQSTM1 function in cellular physiology and disease state.

ProteomeXchange Consortium PRIDE Submission:

Submission details:

Project Name: Proximity labeling reveals dynamic changes in the SQSTM1 protein network.
Project accession: PXD047725
Project DOI: Not applicable

KEYWORDS

SQSTM1, p62, proximity labeling, TurboID, autophagy, tau, MAPT, protein aggregation

INTRODUCTION

Sequestosome 1 (SQSTM1), commonly referred to as p62, is a selective autophagy receptor that recognizes and targets specific cellular cargo for degradation, such as misfolded proteins and damaged organelles (Jakobi et al., 2020; Ma et al., 2019; Stolz et al., 2014). SQSTM1 acts as an adaptor that couples cargo to the LC3 protein (and other proteins from the ATG8 family) for transport through the autophagic system for degradation(Birgisdottir et al., 2013; Jakobi et al., 2020; Pankiv et al., 2007). In addition to its role in autophagy, SQSTM1 participates in other cellular processes including signal transduction and cellular stress response(Fang et al., 2020; Kalogeropulou et al., 2018; Woo et al., 2022, 2020). These cellular processes involve dynamic interactions via multiple discrete SQSTM1 functional domains: Phox and Bem1 (PB1), ZZ-type zinc finger, TRAF-6 binding domain, KEAP1-binding region, LC3-interacting region (LIR) and the ubiquitin-associated domain (UBA). SQSTM1 localization is predominantly cytosolic, however; SQSTM1 has also been detected in the nuclear compartment and implicated as a nuclei-to-cytosol shuttle for ubiquitinylated nuclear proteins(Pankiv et al., 2010).

Proteins often operate as part of complex molecular networks orchestrating a plethora of biological processes (Basu et al., 2021; Gingras et al., 2019). The SQSTM1 protein network exhibits central roles in both cellular proteostasis and pathology (Aparicio et al., 2019; Foster et al., 2021; Liu et al., 2017). The importance of SQSTM1 in catabolic processes (*i.e.* autophagy), including neurodegenerative disorders, cancers, and metabolic syndromes (Liang et al., 2022; Mukherjee et al., 2022; Sánchez-Martín et al., 2019; Yu et al., 2021). Thus, characterization of the dynamic SQSTM1 protein interaction network can be used as a tool to probe disease processes broadly, identifying cargo proteins that are ubiquitinated, misfolded or aggregated. Elucidating SQSTM1 protein networks in normal and disease states could provide insights into the evolution of pathological processes, broadening understanding of cellular mechanisms underlying proteostasis and potentially identifying novel disease markers and therapeutic targets.

Targeted proximity labelling has emerged as an innovative proteomic strategy to explore protein-protein interactions. Unbiased enzyme-based approaches confer the advantage of capturing macromolecular interactions within a near native spatial and temporal cellular milieu (Basu et al., 2021). Notably, fusion of the engineered biotin ligase TurboID to a target protein confers biotinylation of other physically proximal proteins which can subsequently be identified by tandem mass spectrometry (Tess C Branon et al., 2018; Cho et al., 2020b, 2020a; Wei et al., 2021).

In this study, we generated and characterized a TurboID-based SQSTM1 chimeric protein to probe SQSTM1 dynamics in native and pathological contexts. The resulting networks reveal large-scale remodeling of SQSTM1 protein cargo in response to pathological states.

Results

Proximity labeling of SQSTM1 protein network

The autophagy receptor SQSTM1 interacts with many proteins under both basal and stress conditions, and these interactions take place protein interaction domains that include LIR, PB1, UBA and KIR (Deng et al., 2017a, 2019; Ma et al., 2019). Novel SQSTM1 interacting partners continue to be discovered (Hosp et al., 2015; Sharaf et al., 2019; Zellner et al., 2021). To enhance understanding of the SQSTM1 protein network, we applied a systematic approach centered on proximity labeling and generated a chimeric FLAG-tagged human full-length TurboID::SQSTM1 (Tess C. Branon et al., 2018; Cho et al., 2020b, 2020a).

To test functionality, HEK-293T cells were transduced with lentiviruses (LVs, MOI 2) expressing either FLAG::TurboID (non-specific background control) or FLAG::TurboID::SQSTM1 (Figure 1A). Consistent with expectation, immunofluorescence analysis of the FLAG epitope demonstrated that FLAG::TurboID::SQSTM1 fusion formed intracellular bodies, a characteristic feature of the native SQSTM1 protein (Figure 1B). In contrast, FLAG::TurboID control protein displayed a dispersed intracellular expression pattern, similar to that observed in prior studies (Cha-Molstad et al., 2017; Jakobi et al., 2020). Imaging the enzymatic biotinylating activity of the FLAG::TurboID::SQSTM1 fusion construct showed a pattern of biotinylation that selectively co-localized with SQSTM1 positive structures (Fig. 1B). In contrast, the FLAG::TurboID control protein exhibited a dispersed pattern, similar to that observed with the anti-FLAG antibody (Figure 1B).

We used Streptavidin-loaded magnetic beads to pull down labelled proteins from LV-transduced HEK-293T cells expressing either vector-only 'Vo', FLAG::TurboID::SQSTM1 or FLAG::TurboID constructs. We subsequently identified labeled proteins by high performance liquid-chromatography coupled to Orbitrap tandem mass spectrometry (LC-MS/MS) (Figure 1C). Following the precision proteomics analysis, we used hierarchical clustering to reveal proteins that were labeled preferentially by FLAG::TurboID::SQSTM1 compared to FLAG::TurboID (Figure 1D). Quantitative comparisons demonstrated that FLAG::TurboID::SQSTM1 enriched a diverse array of 319 cellular proteins, including known SQSTM1 interacting partners like KEAP1, PRKCI, NBR1, Ubiquitin and others (Figure 1E and Supplementary Table 1, Sheet 2).

We cross-referenced with previously annotated interactors comprising the BioGRID-SQSTM1 dataset (Oughtred et al., 2021). This overlap highlighted 83 proteins between these two interactome datasets. In addition, FLAG::TurboID::SQSTM1 construct labeled an additional 236 novel proteins that were not previously described (Figure 1F, Venn diagram). Functional enrichment analysis of gene ontology annotation terms associated with the 236 unique proteins demonstrated an enrichment for factors linked to translation and the cell cycle (Figure 1F, left panel), whereas the overlapping subset of 83 proteins were associated with autophagy and catabolic processes typically associated with core functions (Figure 1F, right panel).

SQSTM1 proximity labeling identifies known and novel SQSTM1 interactors

To validate some of the interactors from the SQSTM1 network recovered by FLAG::TurboID::SQSTM1 (Figures 1D and 1E), we performed independent co-immunoprecipitation experiments. After transducing HEK-293T cells with LVs expressing either Vo, FLAG::TurboID or FLAG::TurboID::SQSTM1, biotinylated proteins were pulled-down and resolved by immunoblotting. As seen in Figure 2A, endogenous KEAP1, endogenous SQSTM1 and ubiquitin were detected preferentially with FLAG::TurboID::SQSTM1 compared to the FLAG::TurboID control.

SQSTM1 links ubiquitinylated proteins to autophagosome-anchored proteins (*e.g.* LC3B, GABARAP and other members from the ATG8 gene family) through its LIR domain (Goold et al., 2013; Johansen and Lamark, 2019; Pankiv et al., 2007). To test whether FLAG::TurboID::SQSTM1 preserves an active LIR domain, both endogenous and ectopically expressed LC3B protein were monitored in HEK-293T cells by immunofluorescence and streptavidin pull-down, respectively. Orthogonal projections demonstrated that both FLAG::TurboID::SQSTM1 and endogenous LC3B co-localized in the same compartment (Figure 2B). In addition, HEK-293T cells expressing either TurboID or TurboID::SQSTM1 were transfected with HA::LC3B, biotinylated proteins were pulled-down, and the HA-tag (HA::LC3B) was then determined by Western-blot.

As expected, the interaction of HA::LC3B and TurboID::SQSTM1 was greater compared to HA::LC3B and TurboID interaction (Figure 2C). Therefore, these observations suggest that FLAG::TurboID::SQSTM1 preserves its SQSTM1 functional domains PB1, LIR, KIR, and UBA.

The SQSTM1 interactome dataset (Figure 1F) also identified 236 previously unknown SQSTM1 interacting proteins. From this dataset, we selected SYNRG and AGO2 for validation based on their strong signals (Figure 1E). To corroborate these interactions, we immune-precipitated soluble protein lysates from HEK-293T cells transfected with a plasmid expressing epitope (HA) tagged SQSTM1, and analyzed the co-purifying proteins by Western-blot. Both SYNRG and AGO2 co-purified with SQSTM1 (Figure 2D). Thus, our proximity proteomics screen uncovered known SQSTM1 protein interactors in HEK-293T cells.

Acute proteasomal inhibition modifies the SQSTM1 protein network

SQSTM1 facilitates degradation of ubiquitinylated proteins (Berkamp et al., 2021; Cohen-Kaplan et al., 2016). To assess how the SQSTM1 interactome changes with ubiquitin enrichment, we investigated the interaction network of FLAG::TurboID::SQSTM1 ± proteasomal inhibition with the small molecule inhibitor MG132 (Rondon-Ortiz et al., 2017). FLAG::TurboID::SQSTM1-transduced HEK-293T cells were co-treated with biotin and either MG132 (50µM,) or vehicle (DMSO). After 2 hrs treatment, whole cell protein lysates were analyzed by Western Blotting. As expected, ubiquitinylated protein signals were elevated in the cells treated with MG132 (Figure 3A), consistent with inhibition of SQSTM1 cargo processing.

We subsequently performed streptavidin affinity-purification followed by LC-MS/MS to identify the biotinylated proteins. Hierarchical clustering of the enriched proteins indicated that FLAG::TurboID::SQSTM1 treated with MG132 labeled different proteins compared to vehicle alone (Figure 3B). Using a criterion of Log_2 FC(TurboID:SQSTM1_MG132 – TurboID::SQSTM1) > 0.58 and FDR < 0.05, 51 proteins including ubiquitin were significantly enriched from the MG132-treated cells (Figure 3C).

To assess the functional properties of this differential protein subnetwork, we cross-mapped annotations from the String- database . Subsequent visualization revealed 3 functional modules, including “Response to stress” and “RNA binding” (Figure 3D). These results demonstrated that TurboID::SQSTM1 is capable of capturing perturbations within the SQSTM1 interactome when proteostasis is altered.

Tau aggregation alters SQSTM1 protein network in CRL-3275 cells

SQSTM1 protein is an autophagy receptor that facilitates protein degradation of misfolded proteins and protein aggregates. The aggregation-prone protein tau, encoded by the *MAPT* gene, has been found to interact with SQSTM1 in both human brain tissue with tauopathies and in murine transgenic tauopathies models (Drummond et al., 2020; Ono et al., 2022; Piras et al., 2016). Moreover, SQSTM1 overexpression has been found to ameliorate tau pathology in murine models (Xu et al., 2018). Given that FLAG::TurboID::SQSTM1 is capable of recognizing changes in the SQSTM1 interactome when proteostasis is dysregulated, we decided to determine how perturbations of the SQSTM1 protein networks occur in presence of tau aggregates. To achieve this, we used the well-established Tau RD P301S FRET Biosensor CRL-3275 cell line , which emit FRET signal upon exposure to tau fibrils (Holmes et al., 2014). Response of the CRL-3275 cells was evident by imaging; the cells were transduced with FLAG::TurboID::SQSTM1 and then treated with recombinant human P301S-MAPT protein fibrils (500ng/mL) or vehicle control for 24 or 48 hours. Transduced-CRL-3275 cells displayed both FLAG::TurboID::SQSTM1 expression and biotinylated protein signals associated with the FRET signal in the presence of tau fibrils, as determined by immunofluorescence and orthogonal projections of the images (Figures 4B and 4C).

To explore the influence of tau aggregates on the molecular composition of the SQSTM1 protein networks, we transduced CRL-3275 cells with FLAG::TurboID::SQSTM1 and then treated them with recombinant fibrillar P301S-Tau protein (500ng/mL) for 24 and 48 hours prior to addition of biotin (100µM, 2hrs). Biotinylated proteins were detected by immunoblotting and then identified by LC-MS/MS (Figures 5D and 5E). Hierarchical cluster analysis of labeled proteins indicated differential protein enrichment in the SQSTM1-protein network 48hrs post-treatment with fibrillar tau. Quantitative comparison of relative abundance of the sample sets stratified by exposure to fibrillar tau identified 24 and 98 proteins in the SQSTM1 network 24 or 48-hrs post-tau treatment compared to baseline, respectively (Log_2 FC > 0.58, p-value < 0.05, Figures 5F and 5G).

We proceeded to analyze the 98 proteins preferentially detected in the 48 vs 0 hr comparison. The SQSTM1 subnetwork induced by fibrillar tau was then grouped based on functional annotations terms (Figure 5A). Notably, we found that some of these enriched proteins are known MAPT interactors that were not detected in unstressed cells (Supplementary Table 1, Sheet 8). Many of these MAPT interacting proteins are not reported as SQSTM1 interactors in existing datasets (BioGRID-SQSTM1), several of these proteins (*e.g.* P4HB, GPI, and ANXA5) are highlighted in Figure 5A.

Tau aggregation sequesters SQSTM1-interacting proteins in CRL-3275 cells

Calreticulin (CALR) is a chaperone protein that resides in the endoplasmic reticulum (ER). This protein has been reported to interact with SQSTM1 in a process called ER-phagy by two mechanisms: a) an indirect interaction via the ER E3 ligase TRIM13 and b) direct interaction as an N-recognin (Kuijpers et al., 2021; Yoo et al., 2018). Strikingly, CALR was the most abundant biotinylated protein, but showed similar levels of biotinylation ± fibrillar tau (Figure 4G). We independently tested interaction of SQSTM1 with CALR by pulling-down biotinylated proteins from CRL-3275 and immunoblotting (Figure 5B). While both CALR and tau domains (CFP::K18-tau and YFP::K18-tau) were successfully pulled-down, the interactions were not affected by the presence of fibrillar tau.

Although fibrillar tau did not change the amount of CALR interaction with SQSTM1, we hypothesized that it might change the subcellular localization of SQSTM1::CALR interactions. The intracellular localization of CALR was imaged by immunofluorescence in FLAG::TurboID::SQSTM1-expressing CRL-3275 cells was imaged in presence or absence of recombinant tau fibrils (Figure 5C). Strikingly, CALR showed areas of consolidation in cells exposed to tau fibrils; these areas of consolidation co-localized with both FRET signal (tau aggregation) and biotinylated proteins (FLAG::TurboID::SQSTM1) indicating association of CALR, SQSTM1 and tau aggregates (Figure 5C). Thus, aggregation of tau leads to sequestration of SQSTM1, which also leads to sequestration of CALR.

To broaden our assessment, we examined whether tau aggregation sequesters other stress-induced SQSTM1 protein subnetwork members. We proceeded to evaluate the cellular localization of two other cellular proteins, STIP1 and P4HB, each of which exhibited significantly higher association with SQSTM1 in presence of fibrillar tau 48hrs vs 0hrs (Figure 4G). STIP1 was previously proposed to interact with SQSTM1 (Zellner et al., 2021) and was also identified in our dysregulated-proteostasis SQSTM1 protein network (Figure 3C). Likewise, P4HB was also previously described to interact with MAPT (Xu et al., 2013). Both proteins exhibited pronounced changes in intracellular localization in response to the accumulation of aggregated tau, as was observed with CALR (Figure 5C). Importantly, the subcellular patterns of STIP1 and P4HB followed SQSTM1 sequestration in response to the accumulation of tau fibrils and co-localized with the resulting FRET signal (tau aggregation).

Collectively, these experiments demonstrate that SQSTM1 proximity labeling identifies changes in the SQSTM1 protein interaction network in responses to tau aggregation and enables discovery of novel proteins that associate dynamically with the SQSTM1 response.

DISCUSSION

In the current study, we generated the chimeric protein TurboID::SQSTM1 that enables proximity labeling of the SQSTM1 protein interaction network by combining TurboID with full-length human SQSTM1 protein. Using targeted proteomics, this chimeric protein uncovered components of the dynamic SQSTM1 protein network in homeostatic and stress conditions, resulting in the identification of both known and novel SQSTM1 interacting proteins (Figures 1 and 2). The novel SQSTM1 interacting partners include proteins associated with dysregulated cellular-proteostasis or the presence of tau protein aggregates (Figures 3 and 4).

SQSTM1 plays a central role in cellular catabolism by engaging with diverse cellular proteins that are targeted for degradation and shuttling them to the autophagosome. This broad ability to identify substrate binding and intracellular aggregates positions the TurboID::SQSTM1 chimera as an informative tool for interrogating macromolecular changes in the composition and evolution of protein aggregates as they accumulate in disease model systems (Tess C Branon et al., 2018; Cho et al., 2020b; Takano et al., 2020). The TurboID::SQSTM1 chimera also serves as a useful resource to broadly explore SQSTM1 functions in an unbiased manner (Tess C Branon et al., 2018; Cho et al., 2020b; Takano et al., 2020). SQSTM1 protein links ubiquitinylated proteins to autophagosome for degradation (Deng et al., 2017a; Klionsky, 2016), forms biomolecular condensates (Berkamp et al., 2021; Sánchez-Martín et al., 2020; Sun et al., 2018), and interacts with small non-coding RNAs to regulate selective autophagy (Horos et al., 2019). The TurboID::SQSTM1 chimera complements other proximity labeling resources that by enabling comprehensive analysis of SQSTM1 interacting proteins *in vitro* and *in vivo* (Guerroue et al., 2017; Zellner et al., 2021). Use of the TurboID::SQSTM1 chimera will particularly facilitate studies investigating how the SQSTM1-dependent network changes within disease models.

The ability to identify known SQSTM1 interaction partners with TurboID::SQSTM1 proximity profile labeling suggests that addition of TurboID to SQSTM1 construct preserves function of the different SQSTM1 protein domains (PB1, UBA, LIR and KIR; as observed in Figures 1 and 2). This important result suggests that the interactions of the TurboID::SQSTM1 chimeric protein will reflect the normal biology of SQSTM1 when applied to *in vivo* and *in vitro* systems. TurboID::SQSTM1 also identified novel SQSTM1 interacting-proteins, including proteins that are associated with translation (Figure 1F). Some of these translation-associated proteins are RNA-binding proteins that contain intrinsically disordered regions (IDRs). Our dataset identified AGO2, which contains an IDR and is a member of the RNA-induced silencing complex (Figures 1 and 2). The association of RNA binding proteins such as AGO2 with SQSTM1 provides a putative mechanism for the presence of RNA in SQSTM1 bodies and might contribute to the tendency of SQSTM1-bodies to form biomolecular condensates (Berkamp et al., 2021; Sánchez-Martín et al., 2020). SYNRG is another novel protein described in our dataset. SYNRG functions as an adaptor protein between AP-1 to clathrin-associated proteins that potentially mediates the association of SQSTM1 with β-arrestin (Hirst et al., 2005; Woo et al., 2022, 2020) and cannabinoid receptor-2 (Sharaf et al., 2019) Thus, novel proteins labeled by TurboID::SQSTM1 provide important new insights about SQSTM1 biology.

The chimeric protein TurboID::SQSTM1 successfully identified perturbations in the SQSTM1 protein network composition during proteasomal inhibition (Figure 3). UPS inhibition induces the translational

stress response, which is known to alter the function and distribution of RNA binding proteins (Wolozin and Ivanov, 2019). Applying the TurboID::SQSTM1 protein in the context of UPS inhibition identified multiple splicing-associated RNA binding proteins, as shown in the sub-set of proteins labelled as 'RNA binding' including DDX47, FUBP3, SFPQ and HNRPF (Figures 3C and 3D). These findings are consistent with previous results indicating that UPS inhibition impacts on alternative splicing and affects the generation of protein variants (Bieler et al., 2012). Our datasets identified an interaction between ARGLU1 and SQSTM1 that occurs selectively in response to proteasomal inhibition (Figures 3C and 3D). Interestingly, ARGLU1 was previously found to be an essential transcriptional co-activator and splicing regulator of glucocorticoid receptor (Magomedova et al., 2019). ARGLU1 and 5 other genes were recently found to be applicable as biomarkers for amyotrophic lateral sclerosis, using weighted gene co-expression network analysis (Daneshafrooz et al., 2022). These results show the utility of TurboID::SQSTM1 protein as a tool for detecting perturbations in SQSTM1 network, using acute UPS inhibition as a model demonstrating how this tool can interrogate cellular stress mechanisms or disease processes.

SQSTM1 protein facilitates the degradation of protein aggregates by linking ubiquitinylated proteins to autophagy (Deng et al., 2017b; Ma et al., 2019; Xu et al., 2018). Our findings demonstrate how SQSTM1 protein networks are altered by the presence of a protein aggregates, such as recombinant fibrillar tau (Figures 4 and 5). The protein networks in Figures 3 and 4 highlight the pathway 'Response to stress', which includes many chaperones commonly associated with misfolded proteins, including both cytoplasmic chaperones (STIP1, HSPB1, HSPA4, HSPA1B, etc.) and ER resident chaperones (CALR, P4HB, HSPA5 and others). The co-chaperone STIP1 is a stress-induced gene that has an essential role presenting protein substrates to HSP90. A proteomic dataset recently reported that the STIP1-SQSTM1 interaction is elevated during autophagy inhibition (Zellner et al., 2021). STIP1 was also recently proposed to be a potential druggable target for neurodegeneration (Bhattacharya and Picard, 2021). These results show how the TurboID::SQSTM1 protein can be used to identify SQSTM1 interactors that function in protein degradation and the 'Response to stress' pathways (Zellner et al., 2021).

The interaction of tau protein and SQSTM1 has been widely described (Fleming et al., 2022; Liu et al., 2017; Menzies et al., 2017). This interaction is proposed to occur through interaction of ubiquitinylated tau with UBA domain from SQSTM1 (Ono et al., 2022), and direct interaction of ZZ domain of SQSTM1 with N region of tau protein via tau proteolysis by N-terminal arginylation (Brower et al., 2013; Yoo et al., 2018). In this report we investigated the perturbation of SQSTM1 network by tau aggregation using CRL-3275 cells (Holmes et al., 2014; Reilly et al., 2017). The resulting networks identify multiple known MAPT protein interactors that are recognized by TurboID::SQSTM1 as part of the SQSTM1 network, including CALR, HNRNPA2B1, HSPA5, etc. (Drummond et al., 2020; Jiang et al., 2021). The TurboID::SQSTM1 dataset also describes novel SQSTM1 interactors that appear only in the presence of tau aggregates (*i.e.* P4HB, SYNCRIP, DNAJC7; Figure 5A). Prior studies described multiple SQSTM1 interactors interacting with tau aggregates including LC3B, UBB, UBA52, and CALR (Drummond et al., 2020; Ono et al., 2022; Piras et al., 2016). The incomplete overlap between existing datasets and our results might reflect a difference between the relatively simple biology of a HEK cell versus the brain. Focusing on SQSTM1 networks rather than tau networks might also direct attention towards proteins that are in the aggregate but associate more closely with SQSTM1 than with tau protein. Thus, this work highlights potentially preferential interactions among interactors of SQSTM1 and tau.

In summary, we provide this novel and validated resource to explore SQSTM1 protein network. TurboID has the capability to explore protein networks *in vitro* and *in vivo,* TurboID::SQSTM1 can then be used in a context-dependent manner to explore SQSTM1 networks (studying tauopathies murine models, cancer research, other neurodegeneration models, cellular-specific SQSTM1 network behavior, etc.). TurboID::SQSTM1 can also identify novel proteins that can be exploited as novel therapeutic targets (*i.e.* AUTOTAC and PROTAC technologies).

Limitations

TurboID::SQSTM1 offers a broad view of the SQSTM1 protein network. This chimeric protein is an overexpressed system that might affect the protein-protein interactions stoichiometry. For that reason, it is important to further validate the novel proteins with alternatives approaches (*e.g.* immunoprecipitation, proximity ligation assay, surface plasmon resonance, microscale thermophoresis, etc.). The present study presents novel SQSTM1 interactors that can be useful for autophagy research (and protein degradation in neurodegenerative disorders). However, the biological mechanisms of these novel interactors remains to be explored to understand their roles in proteostasis.

Funding

NIH (AG080810, AG050471, AG056318, AG06493 and AG072577) and BrightFocus Foundation (AN2020002) to B.W. Rainwater Charitable Foundation to A.R-O.

Materials and methods

DNA constructs

We generated the DNA construct FLAG::TurboID::SQSTM1 by amplifying human SQSTM1 from Dr. Qing Zhong's plasmid (Addgene#280227(Fan et al., 2010)) and TurboID from Dr. Alice Ting's plasmid (Tess C. Branon et al., 2018) via PCR using Q5 high-fidelity (M0492, NEB). Next, we cloned both amplicons into the pHR-SFFV lentiviral vector (Addgene#79121, (Morsut et al., 2016)) using In-Fusion cloning kit (Takara). We verified the sequences of both constructs pHR-[SFFV/FLAG::TurboID] and pHR-[SFFV/FLAG::TurboID::SQSTM1] using Sanger sequencing. These constructs can be found on Addgene.

Mammalian cell culture and Lentiviral packaging

We maintained HEK-293T (CRL-3216, ATCC) and Tau-RD-P301S-K18 FRET Biosensor CRL-3275, ATCC, (Holmes et al., 2014) cell lines in DMEM supplemented with 10% FBS and 1% penicillin/streptomycin. The cells were grown in plates coated with poly-d-lysine (PDL) and in a humidified environment with 5% CO2. To package lentivirus, we grew HEK-293T cells in PDL-coated 10-cm petri dishes and transfected them with transfer plasmids, psPAX2 (Addgene#12260), and VSV-G (Addgene#8454) at a ratio of 1:1:3, respectively, using Fugene-HD reagent (Promega E2311). Three days later, we harvested and concentrated the lentiviral particles using the LentiX concentrator (Takara #631232) following the manufacturer's protocol. The lentiviral titer was then determined using the Lenti-X p24 rapid titer kit (Takara Cat #632200).

To perform the experiments, HEK-293T and CRL-3275 cells were grown in PDL-coated 6-well plates and transduced with lentiviral particles using a multiplicity of infection value of 2. Subsequently, these cells were passaged into either PDL-coated cover slips, 6-well plates, or 10-cm petri dishes. For HA-LC3B-Myc (Addgene #137757) and HA-SQSTM1 (Addgene #280227) transfections, HEK-293T cells were transfected using Lipofectamine 3000 (Thermo Fisher), following the manufacturer's protocol.

Transduction and Transfection

To perform the experiments, HEK-293T and CRL-3275 cells were grown in PDL-coated 6-well plates and transduced with lentiviral particles using a multiplicity of infection value of 2. Subsequently, these cells were passaged into either PDL-coated cover slips, 6-well plates, or 10-cm petri dishes. For HA-LC3B-Myc (Addgene #137757) and HA-SQSTM1 (Addgene #280227) transfections, HEK-293T cells were transfected using Lipofectamine 3000 (Thermo Fisher), following the manufacturer's protocol.

Biotin labeling, Immunocytochemistry, Immunoblot and Biotinylated proteins-streptavidin pull-down

Transduced Hek-293T cells were treated with biotin (100µM, 2 hours). Next, these cells were placed on ice for 10 minutes. Subsequently, cells were fixed with 4%PFA in PBS for 15 minutes. Fixed cells were permeabilized using ice-cold methanol for 5 minutes, as previously described (Cho et al., 2020b). Cells were then blocked with 5% donkey serum, 5% bovine-serum albumin and 22.52 mg/mL of glycine in PBS-T. Antibodies are described in Table 1.

Following biotin labeling, cells were rinsed with ice-cold PBS twice and lysed in RIPA buffer (0.5% sodium deoxycholate, 1% TritonX100, 0.5% SDS, 1mM EDTA, 150mM NaCl, 50mM Tris-HCl pH 7.5). Protein concentration was determined using BCA assay and 40µg of total proteins were resolved using Western blot. For streptavidin pull-downs, 3 mg of total proteins were pulled-down using Pierce Streptavidin magnetic beads (Cat#88816).

Table 1. Antibodies used in this study

Application	Antibody	Host	Manufacturer	Cat number	Dilution
ICC	FLAG	Mouse	Sigma	F1804	1:200
WB	Streptavidin-HRP	N/A	Thermo Fisher	21126	1:5000
WB	Ubiquitin	Mouse	Cell Signaling	3936	1:2000
WB	FLAG	Mouse	Sigma	F1804	1:2000
WB	GFP	Rabbit	Thermo Fisher	A-11122	1:5000
IP/WB	KEAP1	Rabbit	Cell Signaling	8047S	1:1000
IP/WB	SQSTM1	Rabbit	ABCAM	ab109012	1:10000
ICC	HA	Mouse	BIOLEGEND	901502	1:250
WB/IP	HA	Mouse	BIOLEGEND	901502	1:2000
ICC	LC3B	Rabbit	ABCAM	AB192890	1:100
WB	CALR	Rabbit	ABCAM	ab92516	1:5000
wb	CALR	Rabbit	ABCAM	ab92516	1:5000
ICC	STIP1	Rabbit	ABCAM	ab126724	1:10000
WB/IP	P4HB	Rabbit	ABCAM	ab137110	1:2000
WB/IP	AGO2	Rabbit	ABCAM	ab156870	1:2000
WB/IP	SYNRG	Rabbit	BETHYL BIOSCIENCES	A304-567A	1:2000

WB	Anti Mouse IgG (H+L) Secondary Antibody, HRP	Goat	Thermo Fisher	62-6520	1:5000
WB	Anti Rabbit IgG (H+L) Secondary Antibody, HRP	Goat	Thermo Fisher	62-6120	1:5000
ICC	Streptavidin-DyLight 488	N/A	Vector Labs	SA-5488-1	1:2000
ICC	Streptavidin-DyLight 649	N/A	Vector Labs	SA-5649-1	1:2000
ICC	Alexa Fluor conjugated secondary antibodies	Donkey	Jackson Immunoresearch		1:1000

Immunoprecipitation

HEK-293T cells transiently expressing HA::SQSTM1 were lysed in IP-buffer (0.1% NP-40, 1mM EDTA, 120 mM NaCl, 50mM tris-HCl pH 7.5) on ice. Protein concentration was determined by BCA assay and 2 mg of total protein was taken. Following, 2µg of anti-HA antibody was added to each sample and incubated for 2 hours at 4C. Subsequently, 50µL of Dynabeads Protein G (ThermoFisher Cat#10004D) were added to each sample and the samples were incubated overnight at 4C. Next day, the samples were washed with IP-buffer 3 times (5 minutes each) and samples were eluted in WB loading buffer.

Sample preparation for LC-MS/MS

After cell transduction, cells expressing either FLAG::TurboID or FLAG::TurboID::SQSTM1 were plated in PDL-coated 10-cm dishes. Upon reaching confluency, a subset of the cells was treated with 100 µM biotin 2hrs to induce protein biotinylation. The cells were subsequently lysed in Lysis buffer containing 50mM Tris-HCl (pH 7.5), 150mM NaCl, 1mM EDTA, 0.5% SDS, 1% Triton-X100 and 0.5% sodium deoxycholate. The lysis buffer was supplemented with protease inhibitors (Halt protease inhibitor cocktail, Thermo Fisher # 78429). Protein levels were quantified using a BCA assay kit from Thermo Fisher. Equal protein amounts (3mg) were immunoprecipitated overnight at 4C using Streptavidin Magnetic Beads (Pierce #88816). Following the streptavidin pull down, the beads were washed twice with RIPA buffer, once with KCl 1M, once with Na2CO3 0.1M, once with Urea 2M (in 10mM Tris-HCl, pH 8) and twice with ammonium bicarbonate 50mM as previously described (Cho et al., 2020b)

To perform on-bead digestion, the beads were suspended in 200 µL of 50 mM ammonium bicarbonate and incubated for 30 minutes at room temperature with 40 mM chloroacetamide and 10 mM TCEP to alkylate and reduce the proteins, respectively. The reaction was then quenched using 20 mM DTT. The beads were subsequently digested overnight at 37C with 1 µg of MS-grade trypsin from Thermo Fisher Scientific (Cat#90058). The next day, the digested peptides were collected into new tubes, and the trypsin-digestion reaction was quenched with formic acid (final concentration of 1%). These peptides were then desalted using Pierce C18 columns (Thermo Fisher Scientific, Cat#89870), following the manufacturer's protocol, and finally stored at -80C for further proteomics analysis.

HPLC-ESI MS/MS and Data Analysis

The LC-MS/MS analysis was performed as previously described (Jiang et al., 2021; Webber et al., 2023). In brief, the desalted peptides were reconstituted in 1% formic acid and fractionated using C18 PepMap pre-column (3µm, 100Å, 75mm x 2cm) hyphenated to a RSLC C18 analytical column (2mm, 100 Å, 75 µm x 50cm) High performance nanoflow liquid chromatography-Orbitrap tandem mass spectrometry (LC-MS/MS) were performed using the Easy nLC 1200 system coupled to Q-Exactive HF-X MS (Thermo Scientific). All obtained raw data have been deposited to the ProteomeXchange Consortium via the PRIDE partner repository with the dataset identifier PXD047725(Deutsch et al., 2017; Perez-Riverol et al., 2021)

LC-MS/MS raw data were processed in MaxQuant v1.3.7.0 (Tyanova et al., 2016a) , using the Human proteome (2018_04 Uniprot release of UP000005640_9606) with match between-runs activated. Then, the MaxQuant output file was analyzed in Perseus v2.0.3.0 (Tyanova et al., 2016b) using a modified version of the settings described by the Long Lab (Wei et al., 2021) Briefly, LFQ intensity protein values from all conditions were Log_2 transformed, proteins with at least three quantified values per condition were retained, and missing values were replaced using imputation processing from a normal distribution with a width of 0.3 and a downshift value of 1.8 (these are the default values). Statistical comparisons were performed in Perseus applying two-tailed *t*-test with either a permutation-based FDR of 0.05 or *p*-value less than 0.05. ANOVA was used for a two-dimensional hierarchical clustering considering a permutation-based FDR of 0.05.

Enriched proteins from the comparisons were cross-referenced using the interactome database BioGRID (accessed on 11.21.2021). Additionally, these enriched proteins were used to build protein networks in Cytoscape Version 3.9.1 and this network was sub-clustered with the ClusterMaker2 Version 2.3.2 plugin. Functional annotation terms were determined using ShinyGO Version 0.76.3 (Ge et al., 2019).

References

Aparicio R, Rana A, Walker DW. 2019. Upregulation of the Autophagy Adaptor p62/SQSTM1 Prolongs Health and Lifespan in Middle-Aged Drosophila. *Cell Reports* **28**:1029-1040.e5. doi:10.1016/j.celrep.2019.06.070

Basu A, Ash PE, Wolozin B, Emili A. 2021. Protein Interaction Network Biology in Neuroscience. *Proteomics* **21**:1900311. doi:10.1002/pmic.201900311

Berkamp S, Mostafavi S, Sachse C. 2021. Structure and function of p62/SQSTM1 in the emerging framework of phase separation. *Febs J*. doi:10.1111/febs.15672

Bhattacharya K, Picard D. 2021. The Hsp70–Hsp90 go-between Hop/Stip1/Sti1 is a proteostatic switch and may be a drug target in cancer and neurodegeneration. *Cell Mol Life Sci* **78**:7257–7273. doi:10.1007/s00018-021-03962-z

Bieler S, Hammer E, Gesell-Salazar M, Völker U, Stangl K, Meiners S. 2012. Low Dose Proteasome Inhibition Affects Alternative Splicing. *J Proteome Res* **11**:3947–3954. doi:10.1021/pr300435c

Birgisdottir AB, Lamark T, Johansen T. 2013. The LIR motif - crucial for selective autophagy. *J Cell Sci*, Journal of Cell Science **126**:3237--3247. doi:10.1242/jcs.126128

Branon Tess C, Bosch JA, Sanchez AD, Udeshi ND, Svinkina T, Carr SA, Feldman JL, Perrimon N, Ting AY. 2018. Efficient proximity labeling in living cells and organisms with TurboID. *Nat Biotechnol* **36**:880–887. doi:10.1038/nbt.4201

Branon Tess C., Bosch JA, Sanchez AD, Udeshi ND, Svinkina T, Carr SA, Feldman JL, Perrimon N, Ting AY. 2018. Efficient proximity labeling in living cells and organisms with TurboID. *Nat Biotechnol* **36**:880--887. doi:10.1038/nbt.4201

Brower CS, Piatkov KI, Varshavsky A. 2013. Neurodegeneration-Associated Protein Fragments as Short-Lived Substrates of the N-End Rule Pathway. *Mol Cell* **50**:161–171. doi:10.1016/j.molcel.2013.02.009

Cha-Molstad H, Yu JE, Feng Z, Lee SH, Kim JG, Yang P, Han B, Sung KW, Yoo YD, Hwang J, McGuire T, Shim SM, Song HD, Ganipisetti S, Wang N, Jang JM, Lee MJ, Kim SJ, Lee KH, Hong JT, Ciechanover A, Mook-Jung I, Kim KP, Xie X-Q, Kwon YT, Kim BY. 2017. p62/SQSTM1/Sequestosome-1 is an N-recognin of the N-end rule pathway which modulates autophagosome biogenesis. *Nat Commun* **8**:102. doi:10.1038/s41467-017-00085-7

Cho KF, Branon TC, Rajeev S, Svinkina T, Udeshi ND, Thoudam T, Kwak C, Rhee H-W, Lee I-K, Carr SA, Ting AY. 2020a. Split-TurboID enables contact-dependent proximity labeling in cells. *Proc National Acad Sci* **117**:12143–12154. doi:10.1073/pnas.1919528117

Cho KF, Branon TC, Udeshi ND, Myers SA, Carr SA, Ting AY. 2020b. Proximity labeling in mammalian cells with TurboID and split-TurboID. *Nat Protoc* **15**:3971–3999. doi:10.1038/s41596-020-0399-0

Cohen-Kaplan V, Livneh I, Avni N, Fabre B, Ziv T, Kwon YT, Ciechanover A. 2016. p62- and ubiquitin-dependent stress-induced autophagy of the mammalian 26S proteasome. *Proc National Acad Sci* **113**:E7490–E7499. doi:10.1073/pnas.1615455113

Daneshafrooz N, Cham MB, Majidi M, Panahi B. 2022. Identification of potentially functional modules and diagnostic genes related to amyotrophic lateral sclerosis based on the WGCNA and LASSO algorithms. *Sci Rep* **12**:20144. doi:10.1038/s41598-022-24306-2

Deng Z, Lim J, Wang Q, Purtell K, Wu S, Palomo GM, Tan H, Manfredi G, Zhao Y, Peng J, Hu B, Chen S, Yue Z. 2019. ALS-FTLD-linked mutations of SQSTM1/p62 disrupt selective autophagy and NFE2L2/NRF2 anti-oxidative stress pathway. *Autophagy* **16**:1–15. doi:10.1080/15548627.2019.1644076

Deng Z, Purtell K, Lachance V, Wold MS, Chen S, Yue Z. 2017a. Autophagy Receptors and Neurodegenerative Diseases. *Trends Cell Biol* **27**:491--504. doi:10.1016/j.tcb.2017.01.001

Deng Z, Purtell K, Lachance V, Wold MS, Chen S, Yue Z. 2017b. Autophagy Receptors and Neurodegenerative Diseases. *Trends Cell Biol* **27**:491–504. doi:10.1016/j.tcb.2017.01.001

Deutsch EW, Csordas A, Sun Z, Jarnuczak A, Perez-Riverol Y, Ternent T, Campbell DS, Bernal-Llinares M, Okuda S, Kawano S, Moritz RL, Carver JJ, Wang M, Ishihama Y, Bandeira N, Hermjakob H, Vizcaíno JA. 2017. The ProteomeXchange consortium in 2017: supporting the cultural change in proteomics public data deposition. *Nucleic Acids Res* **45**:D1100–D1106. doi:10.1093/nar/gkw936

Drummond E, Pires G, MacMurray C, Askenazi M, Nayak S, Bourdon M, Safar J, Ueberheide B, Wisniewski T. 2020. Phosphorylated tau interactome in the human Alzheimer's disease brain. *Brain* **143**:awaa223. doi:10.1093/brain/awaa223

Fan W, Tang Z, Chen D, Moughon D, Ding X, Chen S, Zhu M, Zhong Q. 2010. Keap1 facilitates p62-mediated ubiquitin aggregate clearance via autophagy. *Autophagy* **6**:614–621. doi:10.4161/auto.6.5.12189

Fang C, Woo J-AA, Liu T, Zhao X, Cazzaro S, Yan Y, Matlack J, Kee T, LePochat P, Kang DE. 2020. SSH1 impedes SQSTM1/p62 flux and MAPT/Tau clearance independent of CFL (cofilin) activation. *Autophagy* **00**:1--22. doi:10.1080/15548627.2020.1816663

Fleming A, Bourdenx M, Fujimaki M, Karabiyik C, Krause GJ, Lopez A, Martín-Segura A, Puri C, Scrivo A, Skidmore J, Son SM, Stamatakou E, Wrobel L, Zhu Y, Cuervo AM, Rubinsztein DC. 2022. The different autophagy degradation pathways and neurodegeneration. *Neuron* **110**:935–966. doi:10.1016/j.neuron.2022.01.017

Foster AD, Flynn LL, Cluning C, Cheng F, Davidson JM, Lee A, Polain N, Mejzini R, Farrawell N, Yerbury JJ, Layfield R, Akkari PA, Rea SL. 2021. p62 overexpression induces TDP-43 cytoplasmic mislocalisation, aggregation and cleavage and neuronal death. *Sci Rep-uk* **11**:11474. doi:10.1038/s41598-021-90822-2

Ge SX, Jung D, Yao R. 2019. ShinyGO: a graphical gene-set enrichment tool for animals and plants. *Bioinform Oxf Engl* **36**:2628–2629. doi:10.1093/bioinformatics/btz931

Gingras A-C, Abe KT, Raught B. 2019. Getting to know the neighborhood: using proximity-dependent biotinylation to characterize protein complexes and map organelles. *Curr Opin Chem Biol* **48**:44--54. doi:10.1016/j.cbpa.2018.10.017

Goold R, McKinnon C, Rabbanian S, Collinge J, Schiavo G, Tabrizi S. 2013. The LIR motif – crucial for selective autophagy. *J Cell Sci* **126**:3237–3247. doi:10.1242/jcs.126128

Guerroue FL, Eck F, Jung J, Starzetz T, Mittelbronn M, Kaulich M, Behrends C. 2017. Autophagosomal Content Profiling Reveals an LC3C-Dependent Piecemeal Mitophagy Pathway. *Mol Cell* **68**:786--796.e6. doi:10.1016/j.molcel.2017.10.029

Hirst J, Borner GHH, Harbour M, Robinson MS. 2005. The Aftiphilin/p200/γ-Synergin Complex. *Mol Biol Cell* **16**:2554–2565. doi:10.1091/mbc.e04-12-1077

Holmes BB, Furman JL, Mahan TE, Yamasaki TR, Mirbaha H, Eades WC, Belaygorod L, Cairns NJ, Holtzman DM, Diamond MI. 2014. Proteopathic tau seeding predicts tauopathy in vivo. *Proc National Acad Sci* **111**:E4376–E4385. doi:10.1073/pnas.1411649111

Hondius DC, Koopmans F, Leistner C, Pita-Illobre D, Peferoen-Baert RM, Marbus F, Paliukhovich I, Li KW, Rozemuller AJM, Hoozemans JJM, Smit AB. 2021. The proteome of granulovacuolar degeneration and neurofibrillary tangles in Alzheimer's disease. *Acta Neuropathol* **141**:341–358. doi:10.1007/s00401-020-02261-4

Horos R, Bu M, Kleinendorst R, Huber W, Sachse C, Hentze MW. 2019. The Small Non-coding Vault RNA1-1 Acts as a Riboregulator of Autophagy. *Cell*. doi:10.1016/j.cell.2019.01.030

Hosp F, Vossfeldt H, Heinig M, Vasiljevic D, Arumughan A, Wyler E, Consortium the G and ER for AD (GERAD1), Landthaler M, Hubner N, Wanker EE, Lannfelt L, Ingelsson M, Lalowski M, Voigt A, Selbach M. 2015. Quantitative Interaction Proteomics of Neurodegenerative Disease Proteins. *Cell Rep* **11**:1134–1146. doi:10.1016/j.celrep.2015.04.030

Jakobi AJ, Huber ST, Mortensen SA, Schultz SW, Palara A, Kuhm T, Shrestha BK, Lamark T, Hagen WJH, Wilmanns M, Johansen T, Brech A, Sachse C. 2020. Structural basis of p62/SQSTM1 helical filaments and their role in cellular cargo uptake. *Nat Commun* **11**:1--15. doi:10.1038/s41467-020-14343-8

Jiang L, Lin W, Zhang C, Ash PEA, Verma M, Kwan J, Vliet E van, Yang Z, Cruz AL, Boudeau S, Maziuk BF, Lei S, Song J, Alvarez VE, Hovde S, Abisambra JF, Kuo M-H, Kanaan N, Murray ME, Crary JF, Zhao J, Cheng J-X, Petrucelli L, Li H, Emili A, Wolozin B. 2021. Interaction of tau with HNRNPA2B1 and N6-methyladenosine RNA mediates the progression of tauopathy. *Mol Cell*. doi:10.1016/j.molcel.2021.07.038

Johansen T, Lamark T. 2019. Selective Autophagy: ATG8 Family Proteins, LIR Motifs and Cargo Receptors. *J Mol Biol* **432**:80–103. doi:10.1016/j.jmb.2019.07.016

Kalogeropulou AF, Zhao J, Bolliger MF, Memou A, Narasimha S, Molitor TP, Wilson WH, Rideout HJ, Nichols RJ. 2018. P62/SQSTM1 is a novel leucine-rich repeat kinase 2 (LRRK2) substrate that enhances neuronal toxicity. *Biochem J* **475**:1271–1293. doi:10.1042/bcj20170699

Klionsky D. 2016. Guidelines for use and interpretation of assays for monitoring autophagy (3rd edition). *Autophagy* **12**:1--222. doi:10.1080/15548627.2015.1100356

Kuijpers M, Kochlamazashvili G, Stumpf A, Puchkov D, Swaminathan A, Lucht MT, Krause E, Maritzen T, Schmitz D, Haucke V. 2021. Neuronal Autophagy Regulates Presynaptic Neurotransmission by Controlling the Axonal Endoplasmic Reticulum. *Neuron* **109**:299--313.e9. doi:10.1016/j.neuron.2020.10.005

Liang D, Lin W-J, Ren M, Qiu J, Yang C, Wang X, Li N, Zeng T, Sun K, You L, Yan L, Wang W. 2022. m6A reader YTHDC1 modulates autophagy by targeting SQSTM1 in diabetic skin. *Autophagy* **18**:1318–1337. doi:10.1080/15548627.2021.1974175

Liu H, Dai C, Fan Y, Guo B, Ren K, Sun T, Wang W. 2017. From autophagy to mitophagy: the roles of P62 in neurodegenerative diseases. *J Bioenerg Biomembr* **49**:413–422. doi:10.1007/s10863-017-9727-7

Ma S, Attarwala IY, Xie X-Q. 2019. SQSTM1/p62: A Potential Target for Neurodegenerative Disease. *Acs Chem Neurosci* **10**:2094--2114. doi:10.1021/acschemneuro.8b00516

Magomedova L, Tiefenbach J, Zilberman E, Le Billan F, Voisin V, Saikali M, Boivin V, Robitaille M, Gueroussov S, Irimia M, Ray D, Patel R, Xu C, Jeyasuria P, Bader GD, Hughes TR, Morris QD, Scott MS, Krause H, Angers S, Blencowe BJ, Cummins CL. 2019. ARGLU1 is a transcriptional coactivator and splicing regulator important for stress hormone signaling and development. *Nucleic Acids Res* **47**:gkz010-. doi:10.1093/nar/gkz010

Menzies FM, Fleming A, Caricasole A, Bento CF, Andrews SP, Ashkenazi A, Fullgrabe J, Jackson A, Sanchez MJ, Karabiyik C, Licitra F, Ramirez AL, Pavel M, Puri C, Renna M, Ricketts T, Schlotawa L, Vicinanza M, Won H, Zhu Y, Skidmore J, Rubinsztein DC. 2017. Autophagy and Neurodegeneration: Pathogenic Mechanisms and Therapeutic Opportunities. *Neuron*, Neuron. doi:10.1016/j.neuron.2017.01.022

Morsut L, Roybal KT, Xiong X, Gordley RM, Coyle SM, Thomson M, Lim WA. 2016. Engineering Customized Cell Sensing and Response Behaviors Using Synthetic Notch Receptors. *Cell* **164**:780–791. doi:10.1016/j.cell.2016.01.012

Mukherjee S, Maddalena M, Lü Y, Martinez S, Nataraj NB, Noronha A, Sinha S, Teng K, Cohen-Kaplan V, Ziv T, Arandkar S, Hassin O, Chatterjee R, Pirona A-C, Shreberk-Shaked M, Gershoni A, Aylon Y, Elazar Z, Yarden Y, Schramek D, Oren M. 2022. Cross-talk between mutant p53 and p62/SQSTM1 augments cancer cell migration by promoting the degradation of cell adhesion proteins. *Proc Natl Acad Sci* **119**:e2119644119. doi:10.1073/pnas.2119644119

Ono M, Komatsu M, Ji B, Takado Y, Shimojo M, Minamihisamatsu T, Warabi E, Yanagawa T, Matsumoto G, Aoki I, Kanaan NM, Suhara T, Sahara N, Higuchi M. 2022. Central role for p62/SQSTM1 in the elimination of toxic tau species in a mouse model of tauopathy. *Aging Cell* e13615. doi:10.1111/acel.13615

Oughtred R, Rust J, Chang C, Breitkreutz B, Stark C, Willems A, Boucher L, Leung G, Kolas N, Zhang F, Dolma S, Coulombe-Huntington J, Chatr-aryamontri A, Dolinski K, Tyers M. 2021. The BioGRID database: A comprehensive biomedical resource of curated protein, genetic, and chemical interactions. *Protein Sci* **30**:187–200. doi:10.1002/pro.3978

Pankiv S, Clausen TH, Lamark T, Brech A, Bruun J-A, Outzen H, Øvervatn A, Bjørkøy G, Johansen T. 2007. p62/SQSTM1 Binds Directly to Atg8/LC3 to Facilitate Degradation of Ubiquitinated Protein Aggregates by Autophagy*. *J Biol Chem* **282**:24131–24145. doi:10.1074/jbc.m702824200

Pankiv S, Lamark T, Bruun J-A, Øvervatn A, Bjørkøy G, Johansen T. 2010. Nucleocytoplasmic Shuttling of p62/SQSTM1 and Its Role in Recruitment of Nuclear Polyubiquitinated Proteins to Promyelocytic Leukemia Bodies*. *J Biol Chem* **285**:5941–5953. doi:10.1074/jbc.m109.039925

Perez-Riverol Y, Bai J, Bandla C, García-Seisdedos D, Hewapathirana S, Kamatchinathan S, Kundu DJ, Prakash A, Frericks-Zipper A, Eisenacher M, Walzer M, Wang S, Brazma A, Vizcaíno JA. 2021. The PRIDE database resources in 2022: a hub for mass spectrometry-based proteomics evidences. *Nucleic Acids Res* **50**:D543–D552. doi:10.1093/nar/gkab1038

Piras A, Collin L, Grüninger F, Graff C, Rönnbäck A. 2016. Autophagic and lysosomal defects in human tauopathies: analysis of post-mortem brain from patients with familial Alzheimer disease, corticobasal degeneration and progressive supranuclear palsy. *Acta Neuropathologica Commun* **4**:22. doi:10.1186/s40478-016-0292-9

Reilly P, Winston CN, Baron KR, Trejo M, Rockenstein EM, Akers JC, Kfoury N, Diamond M, Masliah E, Rissman RA, Yuan SH. 2017. Novel human neuronal tau model exhibiting neurofibrillary tangles and transcellular propagation. *Neurobiol Dis* **106**:222–234. doi:10.1016/j.nbd.2017.06.005

Rondon-Ortiz AN, Cardenas CLL, Martinez-Malaga J, Gonzales-Urday AL, Gugnani KS, Bohlke M, Maher TJ, Pino-Figueroa AJ. 2017. High concentrations of rosiglitazone reduce mRNA and protein levels of LRP1 in HepG2 cells. *Front Pharmacol* **8**. doi:10.3389/fphar.2017.00772

Sánchez-Martín P, Saito T, Komatsu M. 2019. p62/SQSTM1: 'Jack of all trades' in health and cancer. *FEBS J* **286**:8–23. doi:10.1111/febs.14712

Sánchez-Martín P, Sou Y, Kageyama S, Koike M, Waguri S, Komatsu M. 2020. NBR1-mediated p62-liquid droplets enhance the Keap1-Nrf2 system. *Embo Rep* **21**:e48902. doi:10.15252/embr.201948902

Sharaf A, Mensching L, Keller C, Rading S, Scheffold M, Palkowitsch L, Djogo N, Rezgaoui M, Kestler HA, Moepps B, Failla AV, Karsak M. 2019. Systematic Affinity Purification Coupled to Mass Spectrometry Identified p62 as Part of the Cannabinoid Receptor CB2 Interactome. *Front Mol Neurosci* **12**:224. doi:10.3389/fnmol.2019.00224

Stolz A, Ernst A, Dikic I. 2014. Cargo recognition and trafficking in selective autophagy. *Nat Cell Biol* **16**. doi:10.1038/ncb2979

Sun D, Wu R, Zheng J, Li P, Yu L. 2018. Polyubiquitin chain-induced p62 phase separation drives autophagic cargo segregation. *Cell Res* **28**:405--415. doi:10.1038/s41422-018-0017-7

Takano T, Wallace JT, Baldwin KT, Purkey AM, Uezu A, Courtland JL, Soderblom EJ, Shimogori T, Maness PF, Eroglu C, Soderling SH. 2020. Chemico-genetic discovery of astrocytic control of inhibition in vivo. *Nature* **588**:296--302. doi:10.1038/s41586-020-2926-0

Tracy TE, Madero-Pérez J, Swaney DL, Chang TS, Moritz M, Konrad C, Ward ME, Stevenson E, Hüttenhain R, Kauwe G, Mercedes M, Sweetland-Martin L, Chen X, Mok S-A, Wong MY, Telpoukhovskaia M, Min S-W, Wang C, Sohn PD, Martin J, Zhou Y, Luo W, Trojanowski JQ, Lee VMY, Gong S, Manfredi G, Coppola G, Krogan NJ, Geschwind DH, Gan L. 2022. Tau interactome maps synaptic and mitochondrial processes associated with neurodegeneration. *Cell*. doi:10.1016/j.cell.2021.12.041

Tyanova S, Temu T, Cox J. 2016a. The MaxQuant computational platform for mass spectrometry-based shotgun proteomics. *Nat Protoc* **11**:2301–2319. doi:10.1038/nprot.2016.136

Tyanova S, Temu T, Sinitcyn P, Carlson A, Hein MY, Geiger T, Mann M, Cox J. 2016b. The Perseus computational platform for comprehensive analysis of (prote)omics data. *Nat Methods* **13**:731–740. doi:10.1038/nmeth.3901

Webber CJ, Murphy CN, Rondón-Ortiz AN, Spek SJF van der, Kelly EX, Lampl NM, Chiesa G, Khalil AS, Emili A, Wolozin B. 2023. Human herpesvirus 8 ORF57 protein is able to reduce TDP-43 pathology: network analysis identifies interacting pathways. *Hum Mol Genet*. doi:10.1093/hmg/ddad122

Wei W, Riley NM, Yang AC, Kim JT, Terrell SM, Li VL, Garcia-Contreras M, Bertozzi CR, Long JZ. 2021. Cell type-selective secretome profiling in vivo. *Nat Chem Biol* **17**:326–334. doi:10.1038/s41589-020-00698-y

Wolozin B, Ivanov P. 2019. Stress granules and neurodegeneration. *Nat Rev Neurosci* **20**:649–666. doi:10.1038/s41583-019-0222-5

Woo J-A, Yan Y, Kee TR, Cazzaro S, Percy KCM, Wang X, Liu T, Liggett SB, Kang DE. 2022. β-arrestin1 promotes tauopathy by transducing GPCR signaling, disrupting microtubules and autophagy. *Life Sci Alliance* **5**:e202101183. doi:10.26508/lsa.202101183

Woo J-AA, Liu T, Fang CC, Castaño MA, Kee T, Yrigoin K, Yan Y, Cazzaro S, Matlack J, Wang X, Zhao X, Kang DE, Liggett SB. 2020. β-Arrestin2 oligomers impair the clearance of pathological tau and increase tau aggregates. *Proc National Acad Sci* **117**:5006–5015. doi:10.1073/pnas.1917194117

Xu L-R, Liu X-L, Chen J, Liang Y. 2013. Protein Disulfide Isomerase Interacts with Tau Protein and Inhibits Its Fibrillization. *PLoS ONE* **8**:e76657. doi:10.1371/journal.pone.0076657

Xu Y, Zhang S, Zheng H. 2018. The cargo receptor SQSTM1 ameliorates neurofibrillary tangle pathology and spreading through selective targeting of pathological MAPT (microtubule associated protein tau). *Autophagy* **15**:583–598. doi:10.1080/15548627.2018.1532258

Yoo YD, Mun SR, Ji CH, Sung KW, Kang KY, Heo AJ, Lee SH, An JY, Hwang J, Xie X-Q, Ciechanover A, Kim BY, Kwon YT. 2018. N-terminal arginylation generates a bimodal degron that modulates autophagic proteolysis. *Proc Natl Acad Sci* **115**:E2716–E2724. doi:10.1073/pnas.1719110115

Yu F, Ma R, Liu C, Zhang L, Feng K, Wang M, Yin D. 2021. SQSTM1/p62 Promotes Cell Growth and Triggers Autophagy in Papillary Thyroid Cancer by Regulating the AKT/AMPK/mTOR Signaling Pathway. *Front Oncol* **11**:638701. doi:10.3389/fonc.2021.638701

Zellner S, Schifferer M, Behrends C. 2021. Systematically defining selective autophagy receptor-specific cargo using autophagosome content profiling. *Mol Cell* **81**:1337-1354.e8. doi:10.1016/j.molcel.2021.01.009

FIGURES

Figure 1. Proximity labeling of SQSTM1 networks.

A) Outline of the lentiviral constructs FLAG::TurboID and FLAG::TurboID::SQSTM1. B) Immunofluorescence images of HEK-293T cells transduced with both constructs (scale bar = 10µm). C) Outline of the targeted proteomic approach. D) Hierarchical clustering by Z-score intensities of differentially selected proteins in transduced HEK-293T cells. Proteins were selected using ANOVA and a permutation-based FDR <0.05 (n=4). E) Quantitative comparison of transduced-HEK-293T cells TurboID::SQSTM1 vs TurboID using a Log2 FC(TurboID::SQSTM1 – TurboID) of 1 and FDR < 0.05. (n=4). F) Comparison of significantly enriched proteins from Fig.1E with BioGRID-SQSTM1 dataset. GO-BP (Gene Ontology – Biological processes). Data listed in Supplementary Table 1, Sheet 7.

Figure 2. SQSTM1 proximity labelling identifies known and novel SQSTM1 interactors

A) Pull-down of biotinylated proteins from transduced HEK-293T cells. Eluted proteins were detected by Western blot. B) Endogenous LC3B immunofluorescence images of HEK-293T cells transduced with both constructs. Lower panel contains orthogonal projections indicating that FLAG::TurboID::SQSTM1 co-localized with endogenous LC3B. (scale bar = 10µm) C) HA::LC3B interaction with TurboID::SQSTM1 detected by pull-down of biotinylated proteins. HEK-293T cells were previously transduced with TurboID and TurboID::SQSTM1 and then transfected with a HA::LC3B plasmid. D) SYNRG and AGO2 interaction with SQSTM1::HA as determined by co-immunoprecipitation using HEK-293T cells.

Figure 3. Acute proteasomal inhibition alters SQSTM1 protein network.

A) MG132 inhibition of proteasome in HEK-293T cells transduced with the lentiviral constructs. B) Hierarchical clustering by Z-score intensities of differentially selected proteins in transduced HEK-293T cells. Proteins were selected using ANOVA and a permutation-based FDR <0.05 (n=4). C) Quantitative comparison of -HEK-293T cells transduced with TurboID::SQSTM1 in presence or absence of MG132. Using Log2 FC(TurboID::SQSTM1_MG132 – TurboID::SQSTM1) of 0.58 and FDR < 0.05 to be considered significant (n=4). Data listed in Supplementary Table 1, Sheet 3. D) Protein network of significantly enriched proteins from Fig. 3C. Network was subclustered using functional annotation terms. Network legend displays unique interacting proteins during proteasomal inhibition.

Figure 4. Tau aggregation alters SQSTM1 protein networks in CRL-3275 cells

A) Outline of the targeted proteomic approach of CRL-3275 cells transduced with TurboID::SQSTM1 in presence or absence of recombinant P301S-MAPT protein fibrils. B) Immunofluorescence of FLAG, biotinylated proteins and FRET signal from CRL-3275 cells transduced with TurboID::SQSTM1 treated with recombinant fibrillar tau for 24 and 48 hours. C) Orthogonal projections of CRL-3275 cells transduced with TurboID::SQSTM1 and treated with recombinant fibrillar tau for 48 hours. Both FLAG and biotinylated protein signals co-localized with FRET signal. D) Western blot analysis of TurboID::SQSTM1 transduced-CRL-3275 cells treated with recombinant fibrillar tau for 24 and 48 hours. E) Hierarchical clustering by Z-score intensities of differentially selected proteins in TurboID::SQSTM1 transduced-CRL-3275 cells and treated with recombinant fibrillar tau for 24 and 48hrs. Proteins were selected using ANOVA and a p-value <0.05 (n=4). Data listed in Supplementary Table 1, Sheet 4. F and G) Quantitative comparison of CRL-3275 cells transduced with TurboID::SQSTM1 and treated with recombinant fibrillar tau. 24hrs vs 0hrs and 48hrs vs 0hrs. Using Log2 FC of 0.58 and p-value < 0.05 to be considered significant. (n=4) Data listed in Supplementary Table 1, Sheet 5, 6.

Figure 5. Tau aggregation sequesters SQSTM1 interacting proteins in CRL-3275 cells.

A) Protein network of significantly enriched proteins from Fig. 4G. Note that SQSTM1 was not found significant in the dataset from Fig.4G. However, SQSTM1 was added in the network to display the interaction of TurboID::SQSTM1. Network was subclustered using functional annotation terms. Network legend displays unique SQSTM1 interacting proteins un presence of MAPT aggregates. Datasets used in the network legend: BioGRID-human-SQSTM1, BioGRID-human-MAPT, (Drummond et al., 2020; Hondius et al., 2021; Tracy et al., 2022). B) Pull-down of biotinylated proteins of CRL-3275 expressing lentiviral constructs treated with recombinant MAPT fibrils for 48hrs. C, D and E) Immunofluorescence of CALR, STIP1 and P4HB in TurboID::SQSTM1-transduced CRL-3275 cells in presence of recombinant fibrillar tau for 48hrs.

Fig.1 Proximity labeling of SQSTM1 protein networks

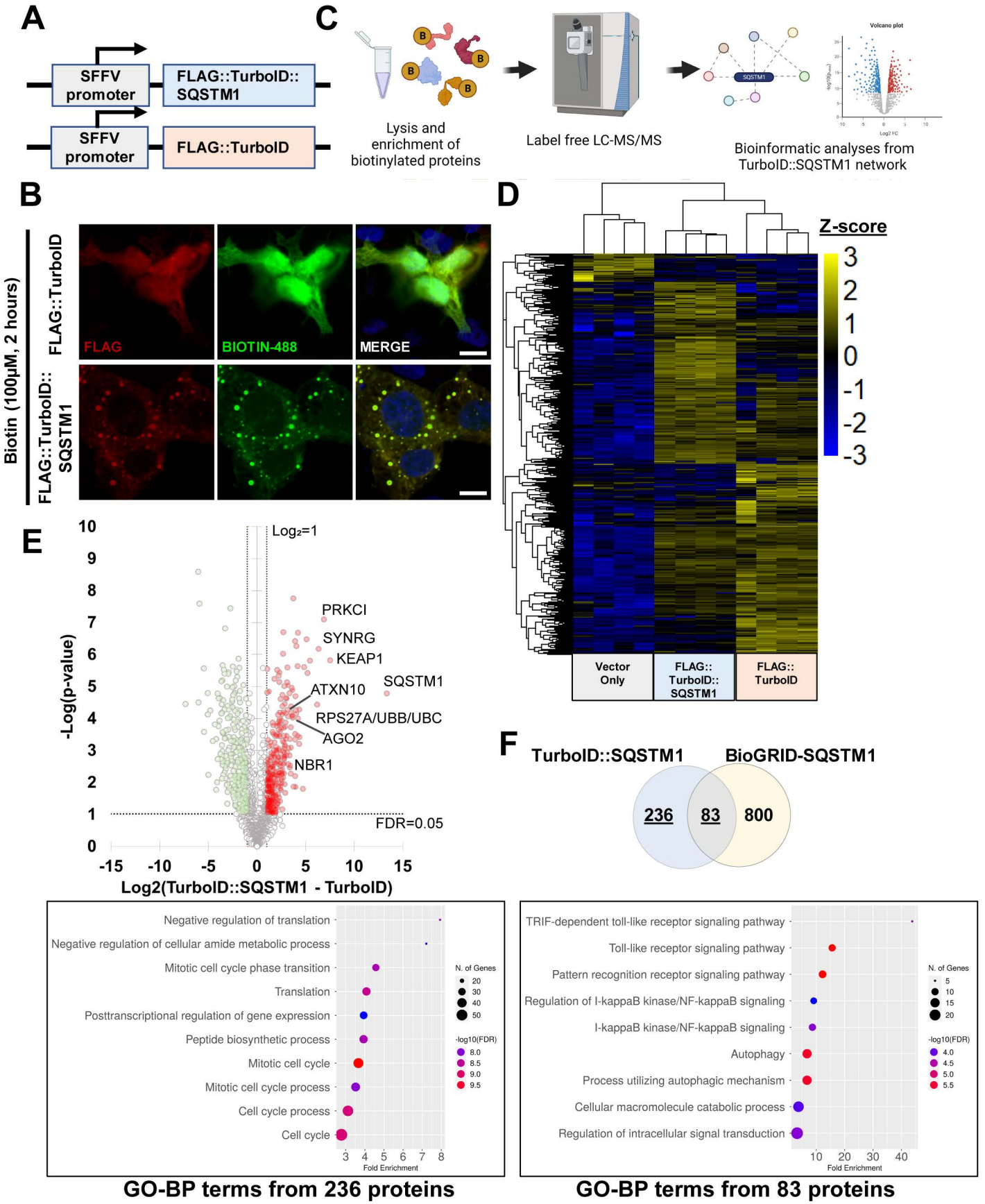

Fig.2 SQSTM1 Proximity labeling identifies *bona fide* and novel SQSTM1 interactors

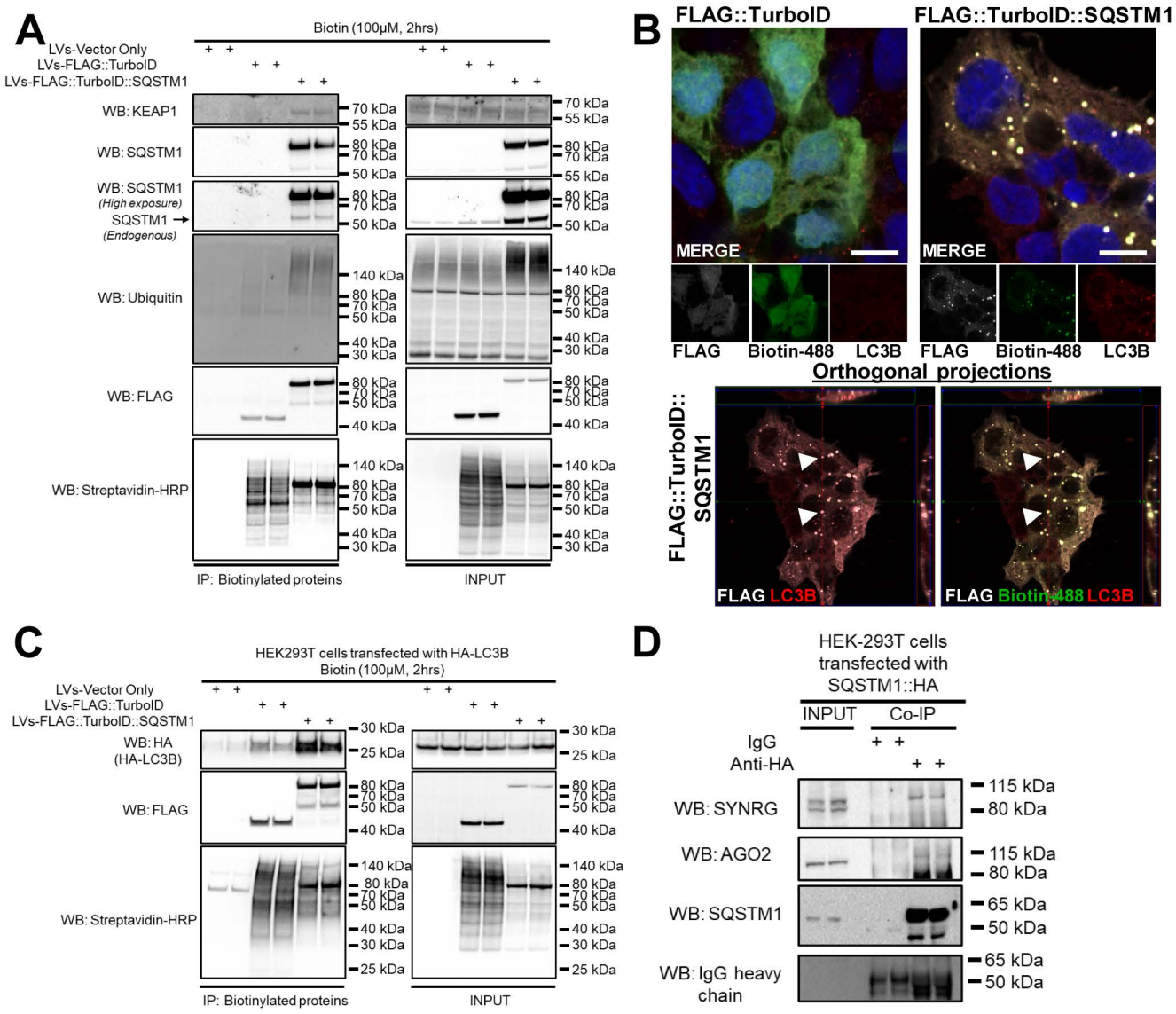

Fig.3 Acute proteasomal inhibition alters SQSTM1 protein network

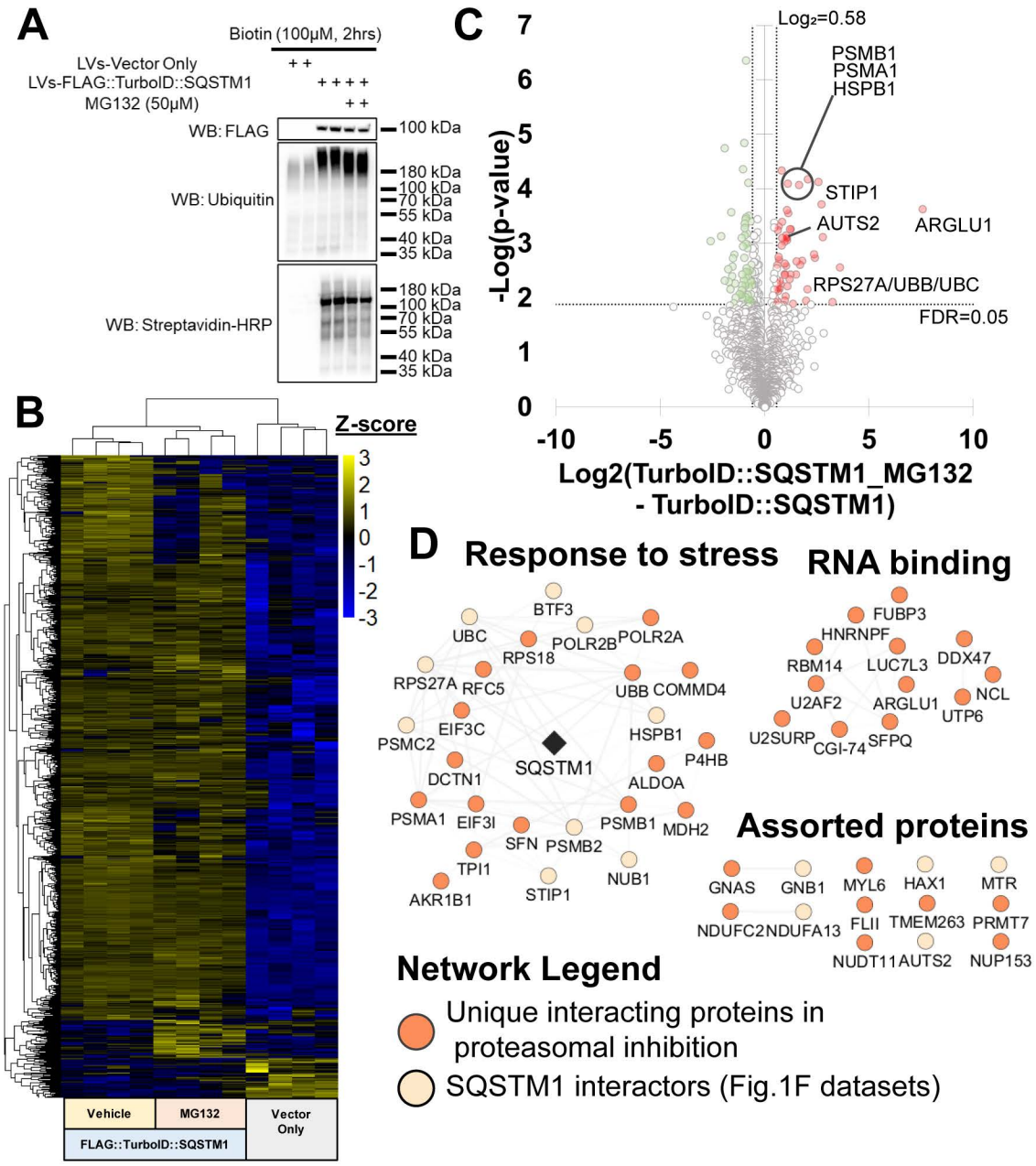

Fig.4 Tau aggregation alters SQSTM1 protein networks in CRL-3275 cells

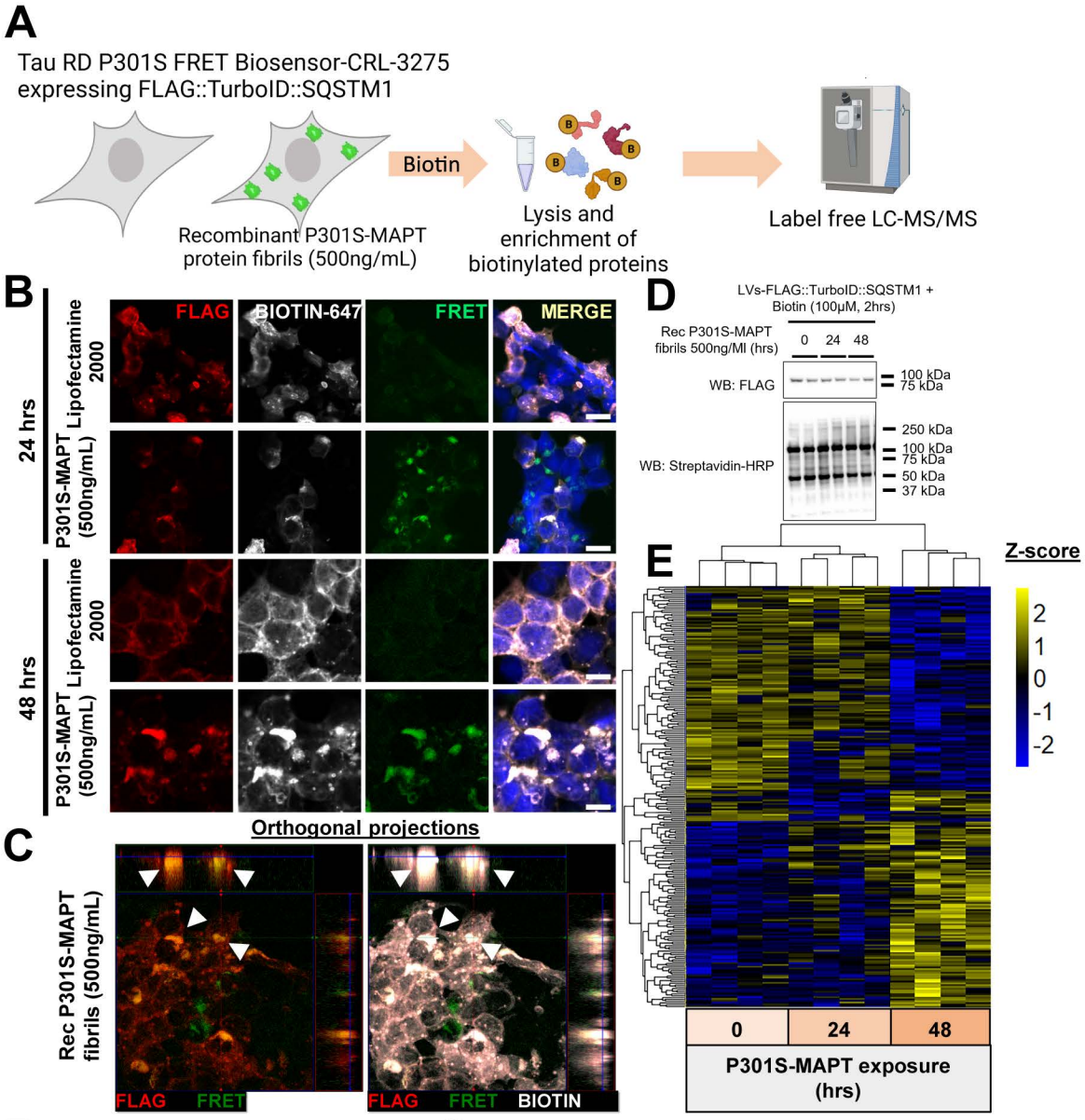

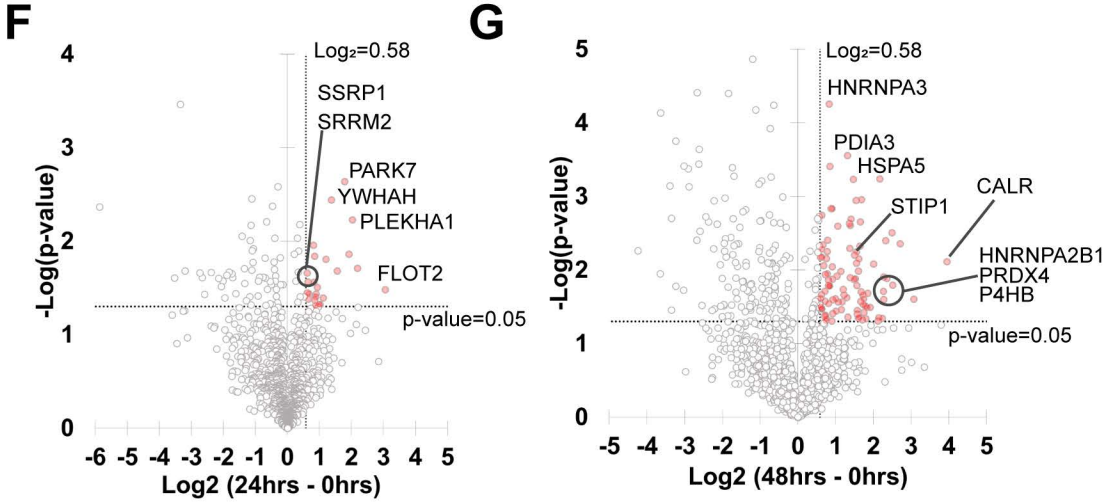
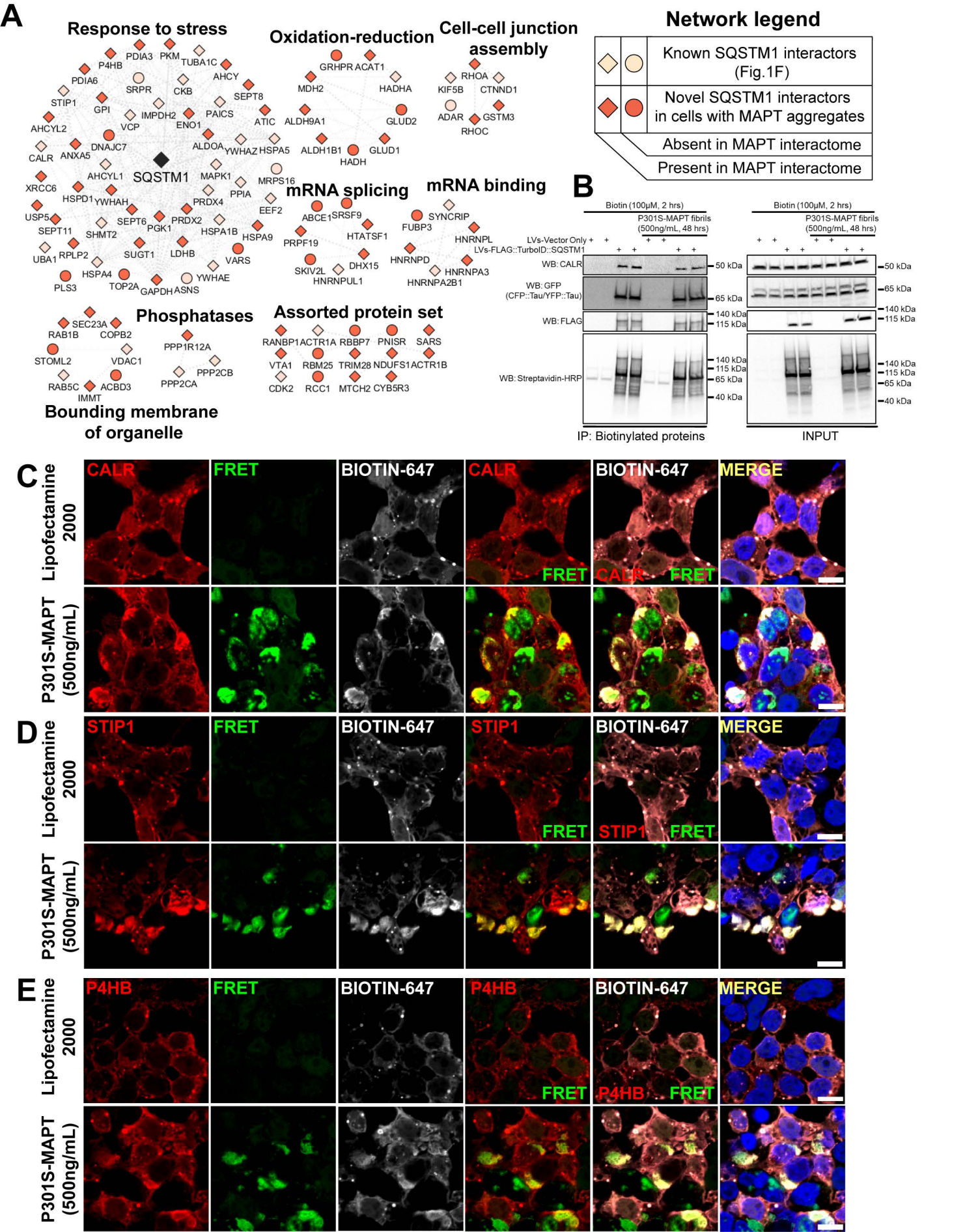
Fig.5 Tau aggregation sequesters SQSTM1 interacting proteins in CRL-3275 cells